Simulative Comparison of Conventional and Secondary Loop Automotive Refrigeration Systems

J C MENKEN, J E KOERNER, T A WEUSTENFELD and K STRASSER
AUDI AG, Germany

J KOEHLER
University of Braunschweig, Germany

Recent attempts to find energy-efficient thermal management systems for electric and plug-in hybrid electric vehicles have led to secondary loop systems. As an alternative approach to meet dynamic heating and cooling demands, these systems reduce the refrigerant charge. Besides advantages such as hermetic encapsulation and a compact, modular design of the refrigeration cycle, secondary loop systems contain an additional layer of thermal resistance. This might influence the system's transient behavior as well as passenger compartment comfort during cool-down or heat-up. Instead of direct refrigerant-to-air heat exchangers, these novel systems are equipped with refrigerant-to-water plate heat exchangers used as indirect condensers and evaporators. The conventional condenser and evaporator in the vehicle front end and in the air handling unit are replaced by water-to-air heat exchangers. This work presents Modelica-based models to examine the transient behaviour of four possible R134a system setups: direct condenser + direct evaporator (conventional refrigeration cycle), direct condenser + indirect evaporator, indirect condenser + direct evaporator, indirect condenser + indirect evaporator (fully integrated secondary loop system). Under defined use cases and environmental conditions, simulations are conducted to compare these four system designs while taking into account the possibility of using the secondary loop system in an efficient heat pump mode for cabin heating.

NOTATION

P	Power	EVAP	Evaporator
E	Energy	COND	Condenser
T	Temperature	ICE	Internal Combustion Engine
$\dot{Q}$	Heat Flow Rate	CHX	Cabin Heat Exchanger
φ	Relative Humidity	pwel	Power Electronics
$\dot{q}_{sol}$	Solar Radiation	emch	Electric Machine
Pr	Prandtl Number	col	coolant
Re	Reynolds Number	ref	refrigerant
Nu	Nusselt Number	amb	ambient
ρ	Density	dEdC	Direct Evaporation/Direct Condensation
p	Pressure	dEiC	Direct Evaporation/Indirect Condensation
d_h	Hydraulic Diameter	iEdC	Indirect Evaporation/Direct Condensation
v	Velocity	iEiC	Indirect Evaporation/Indirect Condensation
t	Time		

INTRODUCTION

For over a century vehicles have been powered by an internal combustion engine (ICE). Growing public awareness of resource shortages and climate change have driven efficiency increases and the development of new propulsion concepts. Customer demands for increasingly efficient vehicles and a comfortable passenger compartment environment create new challenges in heat and energy distribution within the vehicle. Additionally, the move towards greater electrification of the vehicle through hybrid electric vehicles (HEV), plug-in hybrid vehicles (PHEV) and battery electric vehicles (BEV) leads to new thermal management requirements for new components such as energy storage, electric machines and power electronics. These components experience significant transient thermal loading; therefore, much has been invested in order to ensure appropriate and efficient operating conditions [1]. As the number of components requiring active thermal management increases, so do weight, size, cost and system complexity. One method for meeting these thermal management demands while reducing the cost of electric drive systems is through an integrated thermal management system. In this system, the various components (e.g. power elctronic, electric motor, energy storage etc.) are connected via secondary coolant loops to a compact refrigeration cycle as well as to coolant-to-air heat exchangers in the vehicle front end and passenger compartment.

Various applications of secondary loop refrigeration systems can be found in the literature. Wang et al. [2] offer a vaste review on secondary loop refrigeration systems including performance and risk assessment of flammable refrigerants. Applications in the fields of commercial refrigeration, residential air conditioning/heat pumping and mobile air conditioning are presented. The focus in the following will be on vehicle thermal management systems. During the past few years, research in vehicle thermal management via secondary loops has significantly increased. Ghodbane et al. [3] describe a secondary loop system with the HFC refrigerant R152a and demonstrate equal to less cooling performance at a comparable energy consumption compared to the baseline R134a-system. Kowsky et al. [4] present a Central Thermal Management Unit called HPAC (Heat Pump Air Conditioning) for the use in electric and hybrid cars using the battery waste heat as the energy source during the heat pump mode. Downsizing the compact refrigerant cycle to approximately 450mm x 275mm x 225mm reduces the amount of refrigerant and offers packaging flexibility. It is stated that a reduction of refrigerant emissions by at least 50% and an improved electric drive range can be reached. In this presented design, the charge of the tested refrigerant R134a can be reduced by 24% compared to conventional mobile air conditioning systems. The occurring effects in such systems can even be increased by the addition of phase change materials in the secondary loops [5] or using an ice storage [6]. This can be beneficial in order to meet CO_2 emission standards for passenger cars.

This work focuses on the comparison of conventional and secondary loop coolant systems using a simple automotive refrigerant loop containing a compressor, a condenser (refrigerant to air or refrigerant to coolant), an expansion valve, an evaporator (refrigerant to air or refrigerant to coolant) and a refrigerant reservoir (accumulator).

METHODS

Boundary Conditions and Operation Modes

As the requirements of the vehicle thermal management system change over the year depending on the driving cycles and environmental conditions, system evaluation is not a trivial task. In order to use representative data describing operating conditions of the evaluated system, the boundary conditions have to be specified. One system configuration in this work uses the waste heat of electric drivetrain components (battery, electric machine, power electronics) in an integrated secondary loop system. Because of the transient thermal behaviour of the electric drivetrain components and the velocity dependency of the air mass flow rate through the vehicle front end, real world driving cycles must be considered. Additionally, the environmental conditions influence the vehicle's transient behaviour. Therefore, the ambient temperature $T_{air,amb}$, relative humidity $\varphi_{air,amb}$ and solar radiation $\dot{q}_{sol}$ need to be specified.

To describe driving behaviour, the three Artemis driving cycles (urban, road and motorway limited to v=130km/h) are used. Figure 1 shows the velocity profiles over time [7] as well as the calculated drivetrain losses [8]. Taking into account the occurring distribution of urban, sub-urban and motorway profiles, the assumed weighting factors of the three Artemis cycles are shown in Table 1. These factors are based on the general distribution of traveled distances in Germany (0.33 urban, 0.36 road and 0.31 motorway) according to Rumbolz et al. [9] combined with the respective durations of the three given Artemis driving cycles.

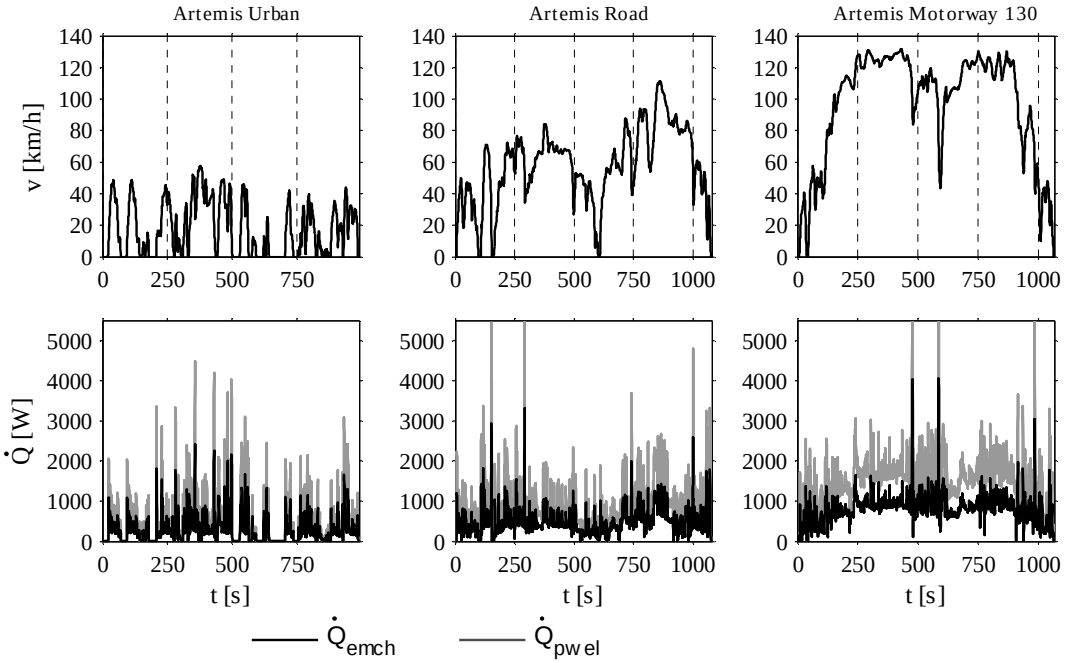

Figure 1 - Velocity profiles of evaluated driving cycles Artemis urban, road and motorway [7]. Drivetrain heat losses of electrical machine and power electronics [8].

Table 1 – Weighting factors for driving cycles Artemis urban, road and motorway [9]**.**

Driving cycle	**Weighting factor**
Artemis Urban	0.68
Artemis Road	0.21
Artemis Motorway 130	0.11

Regarding the ambient conditions, Table 2 displays the values for $T_{air,amb}$, $\varphi_{air,amb}$ and $\dot{q}_{sol}$ including weighting factors [8] used in this work.

Table 2 – Ambient conditions based on European weather data for system evaluation used in this work [8].

Use case	**Weighting factor**	**$T_{air,amb}$** [°C]	**$\varphi_{air,amb}$** [%]	**$\dot{q}_{sol}$** [W/m²]
Heat-up (winter)	0.44	5	75	170
Re-heat (autumn)	0.45	15	64	318
Pull-down (summer)	0.12	30	42	538

For the evaluation of the system configurations, a battery powered electric vehicle is assumed. Because of the lack of an internal combustion engine, the missing heat load during winter and reheat operation mode is either provided by an electrical heater within the supply flow of a coolant-to-air cabin heat exchanger or by a primary refrigerant cycle operated in a heat pump mode. In the following, the operation modes for cabin heat-up, re-heat and cool-down are listed and described in detail. The re-heat operation mode is distinguished by dehumidification of the instream air and subsequent re-heating before entering the passenger compartment.

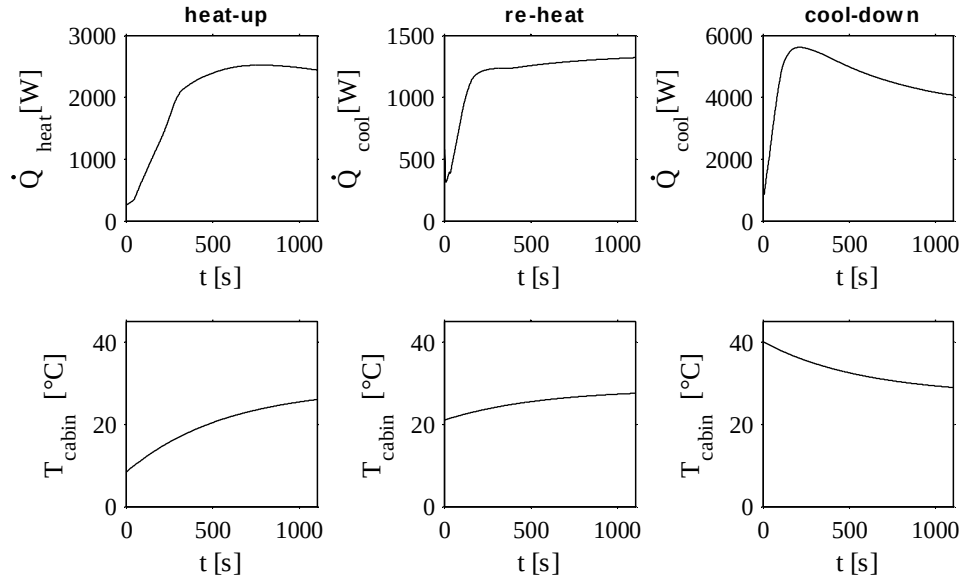

Figure 2 - Air side cooling or heating load at water-to-air or refrigerant-to-air heat exchanger within the air handling unit and respective cabin reference temperatures for heat-up, re-heat and pull-down based on [8].

Based on experiments and preliminary simulation, the cooling or heating load at the refrigerant-to-air or coolant-to-air heat exchangers is predefined as shown in Figure 2. $\dot{Q}_{heat}$ indicates a heat-up of the instream air, whereas $\dot{Q}_{cool}$ indicates the air side cooling load. It should be noted that during re-heat operation, only the cooling load at the first heat exchanger is displayed. It is assumed that the heating load at the second cabin heat exchanger is either supplied by an electric heater or it is assumed that the heat load from the indirect condenser is sufficient. Based on simulational and experimental results, this can be a justified assumption.

System Setup

In order to compare the performance of conventional direct and secondary loop refrigeration systems, four system configurations are examined. Figure 3 shows these different setups containing direct or indirect condensers and evaporators.

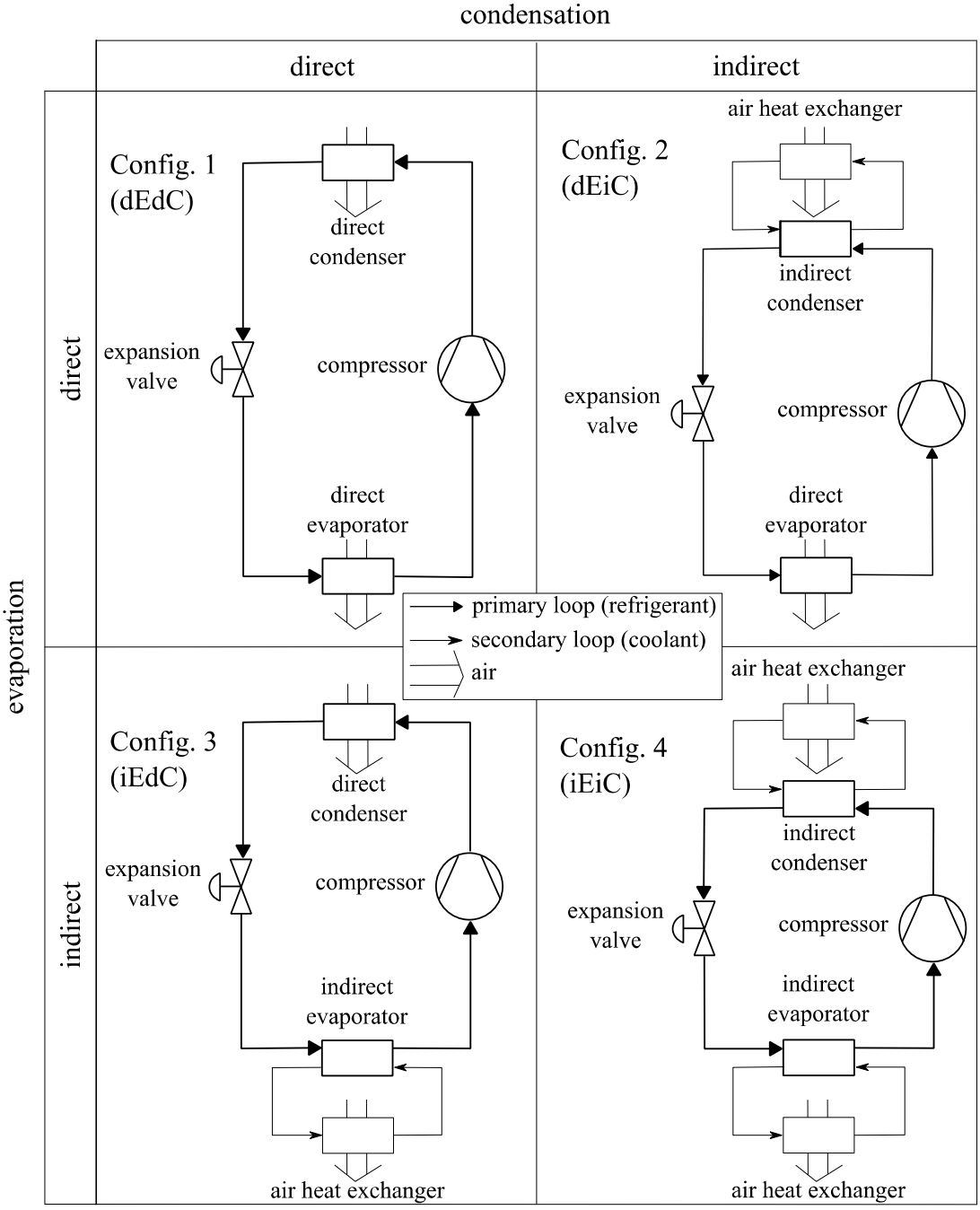

Figure 3 - Overview on examined system configurations.

Configuration 1 (dEdC) represents a conventional system with a refrigerant-to-air evaporator in the air handling unit and a refrigerant-to-air condenser in the front end. Implemented in a vehicle, this configuration would contain the highest refrigerant charge and highest refrigerant side heat losses and pressure drops due to the long hoses and tubes connecting the cycle components within the engine compartment. However, the transient behaviour during cabin cool-down is benchmark due to no additional layer of heat transfer. However, during heat-up and re-heat operation, the entire required heat load must be provided by an electric water heater. Figure 4 shows the simulation setup regarding the air handling unit for all use cases of this configuration with the cabin heat exchanger (CHX) and/or the evaporator (EVAP).

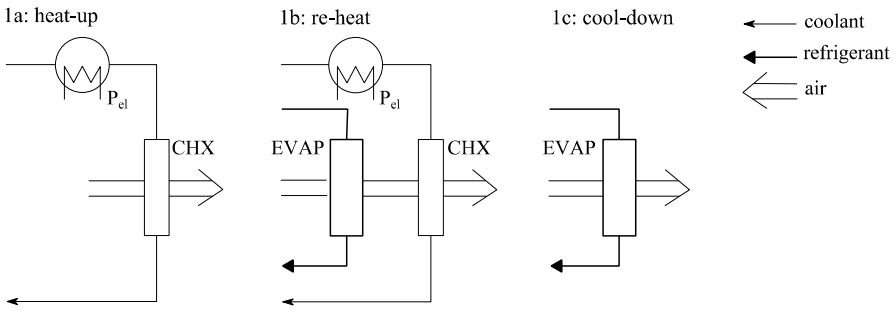

Figure 4 – Air handling unit setup for configuration 1 (dEdC) during heat-up, re-heat and cool-down operation mode.

Configuration 2 (dEiC) consists of a refrigeration cycle with a secondary loop on the high pressure side. With this configuration it is possible to operate the refrigeration cycle in a heat pump mode during re-heat, meaning that the air is cooled down and dehumidified at the direct evaporator (EVAP), and then re-heated with the help of the condensation heat by the cabin heat exchanger (CHX). At first, electric drivetrain components can generally not be used as a heat source at low ambient temperatures (i.e. if the vehicle has been standing overnight.). Figure 5 shows the simulation setup regarding the air handling unit for all use cases of configuration 2 (dEiC).

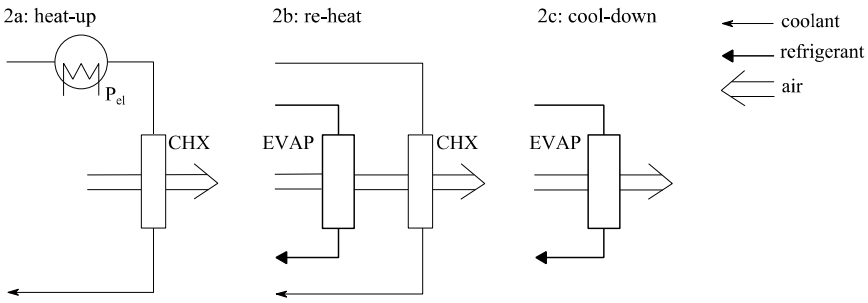

Figure 5 – Air handling unit setup for configuration 2 (dEiC) during heat-up, re-heat and cool-down operation mode.

Configuration 3 (iEdC) consists of a refrigeration cycle with a secondary loop on the low pressure side. With this configuration it is not possible to use the condensation heat during heat-up or re-heat. To cool down the passenger compartment in summer, a cabin heat exchanger is supplied with cold water from the indirect evaporator. Figure 6 shows the simulation setup regarding the air handling unit for all use cases of this configuration.

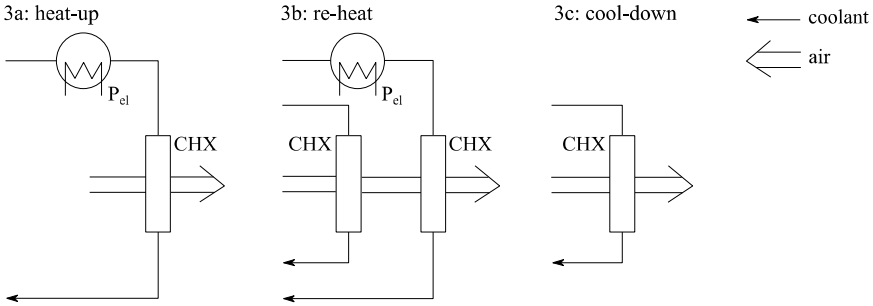

Figure 6 - Air handling unit setup for configuration 3 (iEdC) during heat-up, re-heat and cool-down operation mode.

Configuration 4 (iEiC) consists of a refrigeration cycle with a secondary loop on the high and low pressure side (fully integrated secondary loop system). Due to the fact that all control and energy flow distribution happens on the coolant side, a range of new options like a heat pump mode and the incorporation of electric drivetrain components to the thermal management system emerge. Additionally, the ambient air can be used as heat source during this heat pump mode. Figure 7 shows the simulation setup regarding the air handling unit for all use cases of configuration 4 (iEiC).

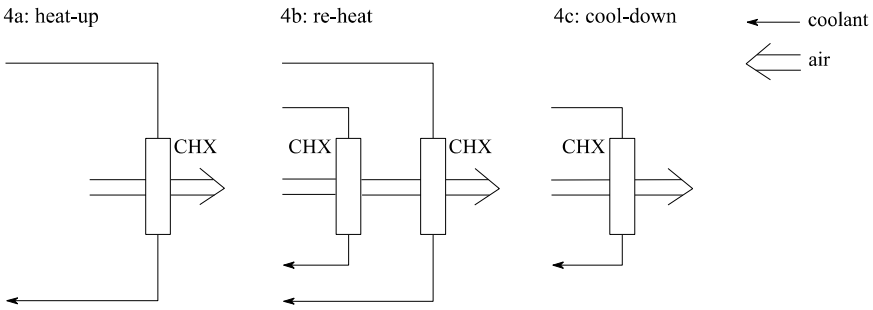

Figure 7 - Air handling unit setup for configuration 4 (iEiC) during heat-up, re-heat and cool-down operation mode.

Based on experimental results and to ensure a high performance of the indirect condenser, all configurations using a secondary coolant loop have a common coolant mass flow rate of $\dot{m}_{col} = 0.2 \frac{kg}{s}$, except during heat up on the high pressure side. To force the pressure to rise on the high pressure side, the coolant mass flow rate is set to $\dot{m}_{col} = 0.03 \frac{kg}{s}$. It would also be possible to use the temperature air flap instead of reducing the coolant mass flow rate.

Modeling and Simulation

All system setups presented in this work are modeled with the TIL Library [10]. They consist of a 34cm³ electrical scroll compressor, a condenser, an electrical expansion valve, an evaporator and a refrigerant reservoir on the low pressure side (accumulator). The systems containing a secondary loop either on the condensing or evaporating side are equipped with coolant-to-air heat exchangers within the air handling unit or the vehicle front end, respectively. Figure 8 exemplarily shows the model of the refrigerant cycle of configuration 4 (iEiC).

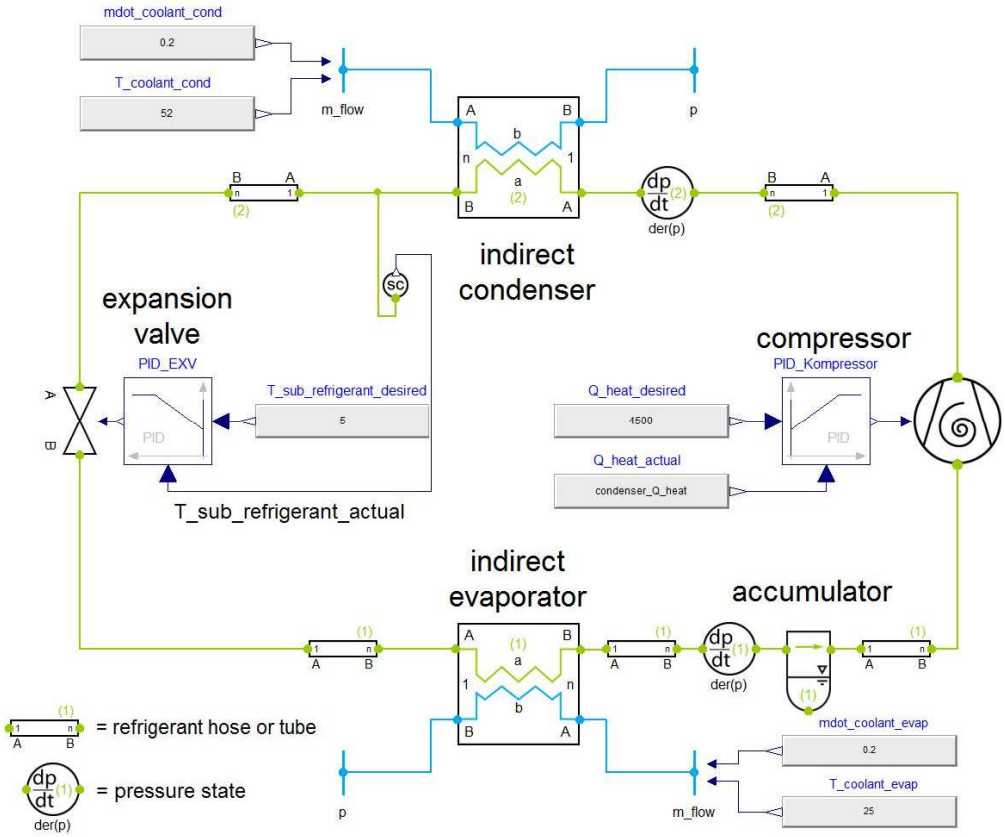

Figure 8 – Refrigerant cycle modeled with the TIL library. Representation of configuration 4 (iEiC).

The compressor is described with a loss-based model according to Schedel et al. [11]. For heat transfer within the evaporator and condenser on the refrigerant side, a plate heat exchanger model is used. The area expansion factor of the plates is obtained by the respective chevron-plate-pattern [12]. Using empirical correction factors of the Dittius-Boelter-Correlation according to Akers/Deans/Crosser [13], the indirect condenser's heat transfer coefficient for Re>50,000 can be calculated as follows (C=5.03, k=0.33):

$$\mathrm{Nu} = \mathrm{C} \cdot \mathrm{Re}^{\mathrm{k}} \cdot \mathrm{Pr}^{1/3}$$

The electric expansion valve is used to control the subcooling of the refrigerant at the condenser outlet. It is modeled with a variable valve opening area according to the Bernoulli-equation:

$$\dot{m}_{ref} = A_{eff} \cdot \sqrt{2 \cdot \rho_{ref,in} \cdot (p_{ref,in} - p_{ref,out})}$$

The refrigerant side heat transfer during evaporation is described with the Lévèque [12] correlation. The Nusselt number is defined as follows:

$$Nu = 1{,}615 \cdot [(\xi \cdot \frac{Re}{64}) \cdot Re \cdot Pr \cdot d_h/l]^{1/3}$$

Consequently, the heat transfer coefficient can then be obtained:

$$\alpha = Nu \cdot \lambda / d_h$$

Due to the design of the accumulator and the oil bleed hole at the bottom of the inner J-tube, the vapour quality of the refrigerant at the accumulator outlet is unsaturated gas [14]. Therefore, a constant outlet vapour quality of $x_{ref,accu,out} = 0.99$ is assumed.
The geometry of the refrigerant to air condenser and evaporator are based on typical automotive components from a compact vehicle. The heat transfer of these components is derived from experimental data.
In order to guarantee comparable conditions, all heat exchangers are modeled with typical pressure loss based on measurements.
All dynamic calculations of the physical properties of the components as well as coolant and refrigerant within the heat exchangers and connections elements are cell-based. This also means that the refrigerant charge has to be chosen appropriately.

A test stand of this primary cycle and the appropriate model validation are presented in previous publications [15], [16].

RESULTS

Figure 9 shows the results of the overall energy consumption for each transient simulation for cabin heat-up, re-heat and cool-down during the respective Artemis driving cycle.

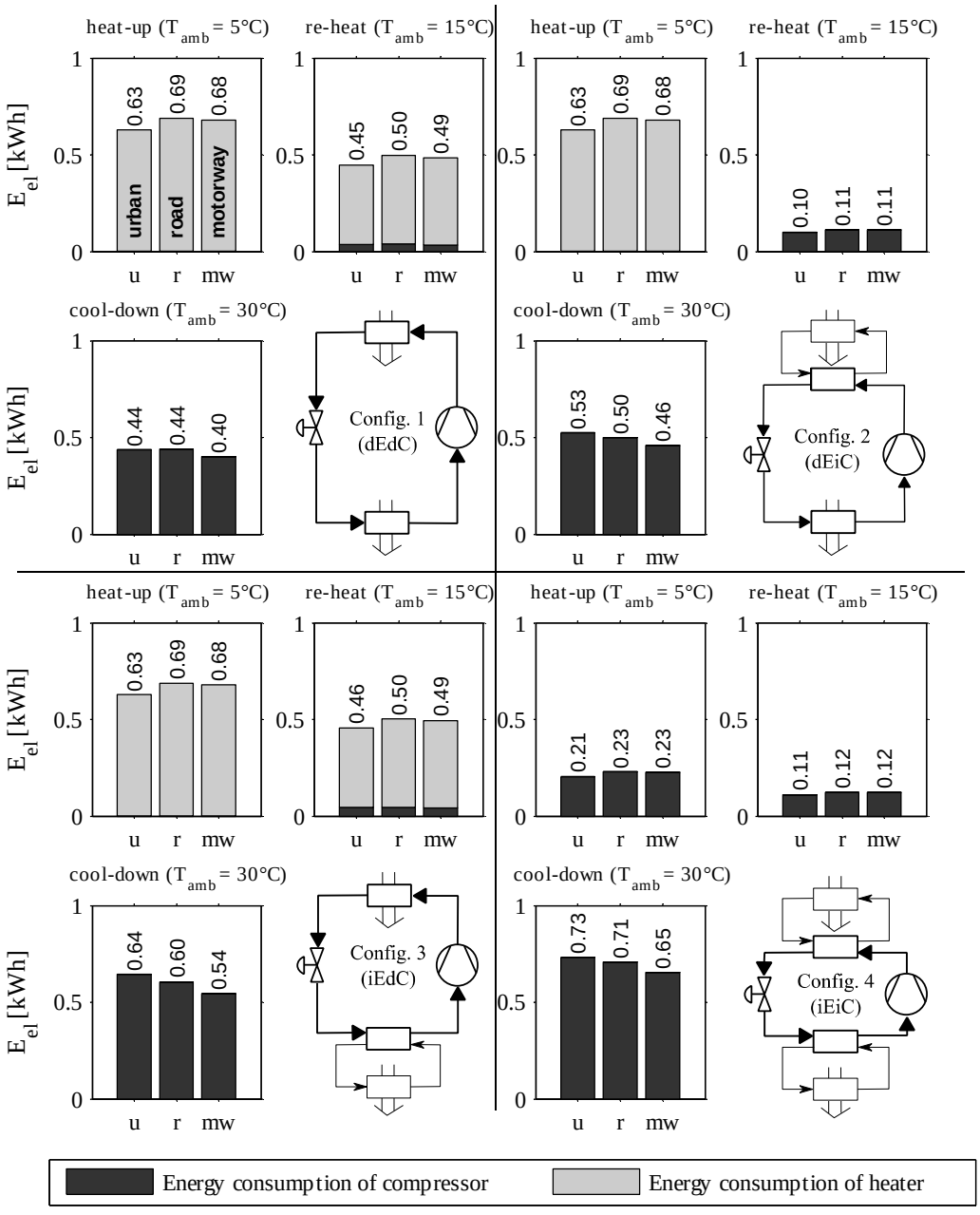

Figure 9 – Results of the energy consumption for all evaluated transient simulations.

Multiplied with the weighting factors for the distribution of driving behaviour shown in Table 1 and the weather date in Table 2, the average energy consumption for an Artemis driving cycle as well as the average energy consumption for each configuration can be obtained from Figure 10.

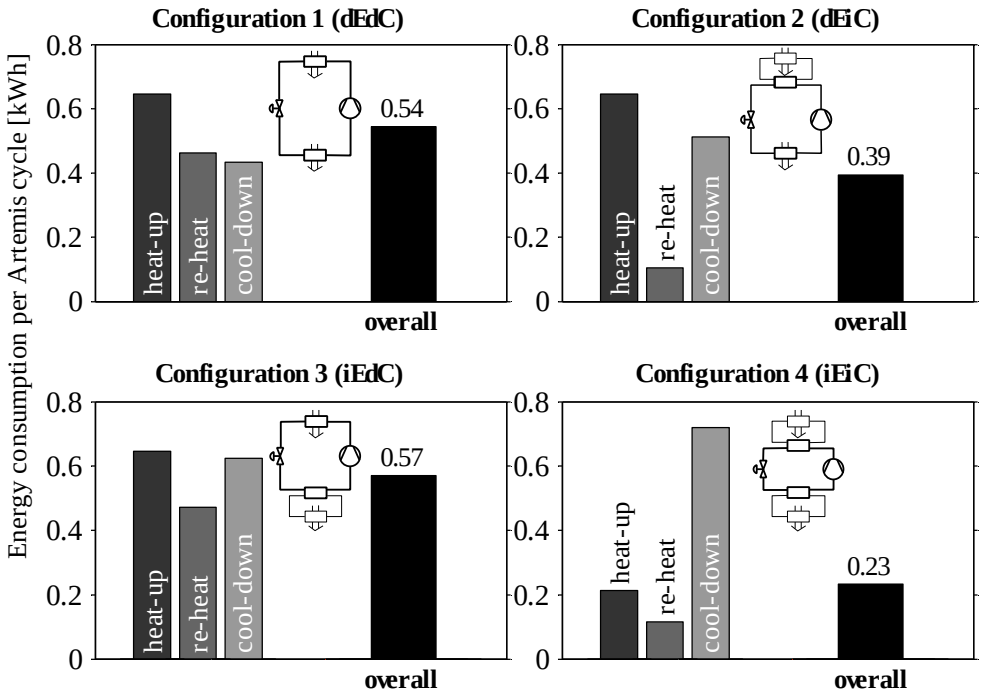

Figure 10 – Weighted energy consumption for an average Artemis driving cycle.

DISCUSSION

During cabin heat-up with configuration 1 (dEdC), 2 (dEiC) and 3 (iEdC), a significantly higher energy consumption can be seen due to the fact that all the heat load has to be brought to the system with an electric heater. In contrast to this, it is possible to operate configuration 4 (iEiC) in an efficient heat pump mode.

During re-heat mode, configurations 2 (dEiC) and 4 (iEiC) show an efficient performance using the condensation heat load to re-heat the dehumidified air.

For cabin cool-down during hot summer conditions, configuration 1 (dEdC) and 2 (dEiC) show the best performance in terms of average energy consumption. This is because of the additional layer of thermal resistance between coolant and refrigerant on the low pressure side. Due to this coolant's thermal mass, a higher amount of energy has to be put up in configuration 3 (iEdC) and 4 (iEiC). It can be seen, that the heat transfer on the low pressure side has a significant influence on the overall system behaviour and can limit the transient performance of the system.

When considering the prevalence (i.e. weighting factors) of the considered environmental conditions, efficiency is crucial especially during heat-up and re-heat mode; however, performance (i.e. time to comfort within the passenger compartment) should not be neglected.

SUMMARY

This work presents a simulative comparison of four different configurations of a refrigerant system using the refrigerant R134a: direct condenser + direct evaporator (conventional refrigeration cycle), direct condenser + indirect evaporator, indirect condenser + direct evaporator, and indirect condenser + indirect evaporator (fully integrated secondary loop system). Under defined use cases and environmental conditions (heat-up, re-heat and cool-down), simulations are conducted to compare the four system designs while taking into account the possibility of using the secondary loop system in an efficient heat pump mode for cabin heating.

It has been shown that a fully integrated secondary loop system can be used to reduce the energy consumption of the thermal management system significantly. This is due to the fact that a heat pump using the waste heat of the electric drive train components can be utilized during winter operation for efficient cabin heat-up at cold start conditions or during re-heat operation.

The next step in the evaluation of secondary loop systems is the inclusion of daily driving patterns, including parking and standing times between driving phases. It is thereby possible to account for storage effects within the secondary coolant loops due to their thermal masses.

REFERENCES

[1] K. Bennion and M. Thornton, „Integrated Vehicle Thermal Management for Advanced Vehicle Propulsion Technologies“, in *SAE 2010 World Congress*, Detroit, Michigan, 2010.

[2] K. Wang, M. Eisele, Y. Hwang and R. Radermacher, „Review of Secondary Loop Refrigeration Systems“, *International Journal of Refrigeration*, Nr. 33(2), 2010.

[3] M. Ghodbane, T. D. Craig and J. A. Baker, „Demonstration of an energy-efficient secondary loop HFC-152a mobile air conditioning system“, in *Final Report for the U.S. Environmental Protection Agency*, 2007.

[4] C. Kowsky, E. Wolfe, L. Leitzel and F. Oddi, „Unitary HPAC system“, *SAE International Journal of Passenger Cars - Mechanical Systems*, Nr. 5(2), 2012.

[5] N. C. Lemke, J. Lemke and J. Koehler, „Secondary Loop Systems for Automotive HVAC Units under different Climatic Conditions“, in *International Refrigeration and Air Conditioning Conference*, Purdue, 2012.

[6] M. Eisele, Y. Hwang and R. Radermacher, "Utilization of Ice Storage in Secondary Loop Automotive Air-Conditioning Systems", in *SAE 2013 World Congress & Exhibition*, Detroit, MI, USA, 2013.

[7] M. Andre, "The ARTEMIS European driving cycles for measuering car pollutant emissions", *Science of the Total Environment*, pp. 79-84, 2004.

[8] T. A. Weustenfeld, J. C. Menken, K. Strasser and J. Koehler, "Central Thermal Management for Electric Vehicles using a fully integrated Primary Loop Refrigeration System", in *Thermal Management System Symposium*, Denver, 2014.

[9] P. Rumbolz, A. Piegsa and H.-C. Reuss, "Messung der Fahrzeug-internen Leistungsflüsse und der diese beeinflussenden Größen im "real-life" Fahrbetrieb", in *VDI-Tagung Innovative Fahrzeugantriebe*, Dresden, 2010.

[10] TLK Thermo GmbH and University of Braunschweig, *TIL Library, version 3.2.3.* 2014.

[11] F. Schedel, G. Suck, S. Foersterling, W. Tegethoff and J. Koehler, "Effizienzbewertungen von Wärmepumpen in Hybridfahrzeugen mit Hilfe der verlustbasierten Modellierung von Scrollverdichtern", in *DKV-Tagung*, Hannover, 2013.

[12] H. Martin, "Pressure Drop and Heat Transfer in Plate Heat Exchangers", in *VDI Heat Atlas*, Heidelberg, Springer Verlag, 2010, pp. Mm1-Mm7.

[13] W. W. Akers, H. A. Deans and O. K. Crosser, „Condensation Heat Transfer within Horizontal Tubes“, *Chemical Engineering Progress Symposium*, Nr. 55, pp. 171-176, 1959.

[14] H. Raiser, T. Heckenberger, W. Tegethoff, J. Koehler and S. Foesterling, "Transient behaviour of R744 vehicle refrigeration cycles and the influence of the suction side accumulator design", *SAE Technical Paper*, no. 2006-01-0162, 2006.

[15] J. C. Menken, T. A. Weustenfeld and J. Koehler, „Experimental Comparison of the Refrigerant Reservoir Position in a Primary Loop Refrigerant Cycle with Optimal Operation“, in *International Refrigeration and Air Conditioning Conference*, Purdue, 2014.

[16] J. C. Menken, T. A. Weustenfeld and J. Koehler, "Reduktion der Kältemittelfüllmenge im Pkw durch den Einsatz von kompakten Kältemittelkreisläufen", in *DKV-Tagung 2014*, Düsseldorf, 2014.